Preliminary Transformation of an NMR Spectrometer into an NMR Imager for Evaluating Fluid Content and Rock Properties of Core Samples

Daryl A. Doughty: ITT Research Institute, National Institute for Petroleum and Energy Research
Nicida L. Maerefat: ITT Research Institute, National Institute for Petroleum and Energy Research

Abstract: A Fourier transform, multinuclear, magnetic resonance spectrometer was modified into a nuclear magnetic resonance imaging (NMRI) machine for use in core analysis studies. The design changes mainly involved the construction of an X-, Y-, Z-gradient coil/RF probe assembly and a gradient control board. Because of its much stronger magnetic field (6.34 Tesla) and higher operating frequency (270 MHz for protons), the modified equipment potentially provides increased sensitivity and resolution over that of medical nuclear magnetic resonance imaging machines. Furthermore, the multinuclear capability of this equipment offers the flexibility of observing more than one type of NMR-sensitive nucleus. Preliminary results obtained with the NMRI machine in imaging water phantoms and water in sand packs and Berea, Cottage Grove, and Cleveland sandstones indicate that high frequencies may not be the best for petrophysical applications of NMRI. Planned modifications include changing the operating frequency from 270 MHz to 60 MHz, constructing a new probe RF coil to operate at 60 MHz, and the inclusion of multislice imaging capability.

INTRODUCTION

Multiphase flow properties and reservoir heterogeneities govern reservoir performance. For a better understanding of multiphase flow in heterogeneous reservoirs, laboratory studies are performed under conditions simulating those found in the reservoirs. The restoration of subsurface reservoir conditions in core samples in the laboratory provides the opportunity to predict reliable multiphase flow and residual oil saturation distribution in the reservoir.

To study fluid flow behavior in porous media, many techniques have been developed for measuring fluid saturations. Saraf and Fatt (1965) were one of the first to use nuclear magnetic resonance (NMR) in laboratory studies of fluid flow in porous media. The advantage of the NMR method for investigating the nature of rock–fluid interactions and monitoring changes in these interactions arises from the number of different NMR parameters available for study, such as variations in chemical shift between fluid types, changes in spin–lattice (T_1) and spin–spin (T_2) relaxation times, and from the nondestructive nature of the experiment, permitting successive studies of the same sample. NMR imaging of rock–fluid interactions permits the investigation of the effects of rock heterogeneities of various types on the distribution of fluids within the rock (Rothwell and Vinegar, 1985).

Recently, many papers describing the use of proton NMR and NMRI to study rock–fluid interactions have been published. Besides Rothwell and Vinegar's paper describing the imaging by NMR of brine-saturated sandstone cores with variations in porosity, Blackband et al. (1986) used NMRI on prepared oil, water, and sand systems to discriminate between various fluid types. Baldwin and Yamanashi (1986) used a medical NMRI instrument to image water and oil in cores. They measured the residual oil from the ratio of NMR intensities before and after waterflooding. Schmidt et al. (1986) used NMR to distinguish between surface adsorbed and bulk water in rock samples. Hall et al. (1986b) applied chemical-shift NMRI to the investigation of Berea sandstone cores partially saturated with water and dodecane. They also reported data on the proton line widths in sandstone and limestone rocks at 80 MHz. Hall and Rajanayagam (1987) reported a technique to obtain thin-slice, chemical-shift imaging of oil and water in sandstone cores. Volk et al. (1987) decribed modified imaging techniques to separately image oil and water in biological samples, but their techniques have not been applied to petrophysical samples.

The first published application of NMRI was by Lauterbur (1973). He used a 60 MHz, high-resolution NMR spectrometer fitted with auxiliary gradient coils to produce the horizontal magnetic field gradients, and mechanically rotated the sample to obtain several projections to reconstruct the image (Lauterbur, 1974). More recently, Hall et al. (1986a) have reported the construction of a gradient coil assembly for an existing NMR probe to obtain NMRI using a 270 MHz superconducting spectrometer. Mareci et al. (personal communication) described a pulse gradient controller driven by the NMR spectrometer pulse programmer to produce magnetic field gradients using the existing shim coils of NMR spectrometers or auxiliary gradient coils.

Several firms market NMRI instruments mainly for medical use, but more recently for more general research purposes. However, these instruments are very expensive and require large amounts of laboratory space. Several NMR spectrometer companies have recently offered im-

aging accessories for their high-resolution instruments, which are also fairly expensive. We constructed our own NMRI modifications for our JEOL GX-270, 270 MHz NMR spectrometer because an imaging accessory was not available for our instrument. This paper presents a brief discussion of NMR imaging theory, the basic modifications we made to achieve imaging capability on our spectrometer, and some of our preliminary NMRI results.

NMRI THEORY

Certain types of nuclei (the primary one for imaging purposes being the proton) possess the property of nuclear spin and a resulting magnetic moment. When placed in an external magnetic field, these nuclear magnetic moments, normally randomly oriented by thermal agitation, tend to align with the external field and produce a bulk magnetic moment (Harris, 1983). The torque exerted on these nuclei by the external field causes their spin axis to precess about the external field direction at a frequency in the radio frequency (RF) region of the spectrum that is characteristic for the particular type of nuclei and is proportional to the strength of the external field.

If the strength of the external magnetic field is homogeneous across the sample, then every particular type of proton in the sample (e.g., water) would have the same frequency, and in a high-resolution NMR experiment would produce a very sharp line in the spectrum at its characteristic frequency. This spectrum would contain information about the types of protons in the sample (e.g., whether they were in oil or water), but would contain no information about their position within the sample. If a linear magnetic field gradient is superimposed on the uniform external field, then the field strength would vary linearly across the sample in the direction of the gradient. The NMR frequency would likewise vary linearly across the sample in this direction, and instead of a single sharp line in the spectrum for each type of proton there would be an envelope of frequencies whose shape would be determined by the shape of the sample and the distribution of protons within the sample (Dumoulin, 1987). By applying gradients in three orthogonal directions, the position of the protons within the sample could be mapped in three dimensions.

Modern NMR spectrometers generally use Fourier transforms (FT) to convert information on the decay and precession of the bulk magnetic moment as a function of time into frequency spectrum information, which gives the quantities of the various types of protons in the sample as a function of their frequency or chemical shift. These data are obtained by placing the sample inside an RF coil, which generates an RF magnetic field orthogonal to the main external field. This field, at the appropriate RF frequency, tips the bulk magnetic moment of the sample away from the main field direction (normally called the Z-axis) towards the X–Y plane. If this RF pulse lasts just long enough to tip the bulk magnetic moment into the X–Y plane, it is called a 90° pulse. A 180° pulse would invert the moment into the negative Z direction. After the 90° pulse, the precessing bulk magnetic moment generates a signal in the RF coil that decays in amplitude by two processes: T_1 (longitudinal or spin–lattice) relaxation and T_2 (transverse or spin–spin) relaxation. T_1 relaxation involves a transfer of energy between the precessing spins, and the energy lattice of the sample as the spins reestablish their equilibrium bulk magnetic moment parallel to the external field. T_2 relaxation is a phase effect in which, because of local magnetic field inhomogenities, some spins precess about the external field faster or slower, causing them to fan out in the X–Y plane until there is no net signal when they become evenly distributed about the Z-axis.

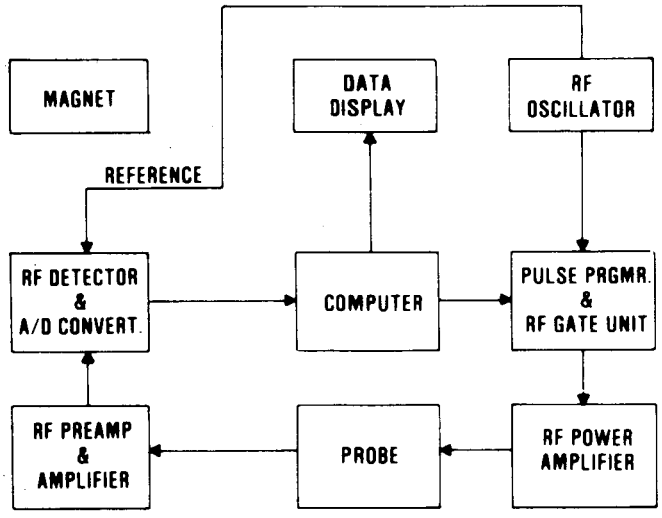

Figure 1: Block schematic diagram of FT-NMR spectrometer.

SPECTROMETER MODIFICATIONS

Figure 1 shows the typical components found in a FT-NMR spectrometer. The probe holds the sample centered in the magnetic field and contains RF coils to irradiate the sample and detect the resulting signal. The magnet contains shim coils to permit adjusting the main field to achieve maximum field homogeneity. The computer controls the spectrometer through the pulse programmer to generate the RF pulses and switch on the RF detector to capture the signal. The computer also digitizes the signal and Fourier transforms it to obtain the NMR spectrum.

To convert an NMR spectrometer into an NMR imager, several modifications are required. The spectrometer must be modified to generate linear magnetic field gradients in three orthogonal directions across the sample region within the main magnetic field. These gradients can be generated by using the spectrometer X, Y, and Z shim coils or, more conveniently, by providing auxiliary gradient coils that will handle larger currents and generate

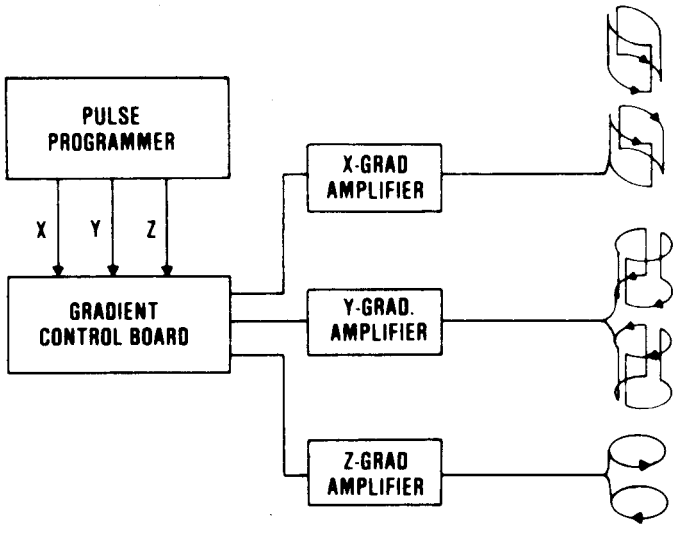

Figure 2: Spectrometer modifications required for X-, Y-, and Z-gradient control. (The three gradient coils shown separately at right are concentric in actual use.)

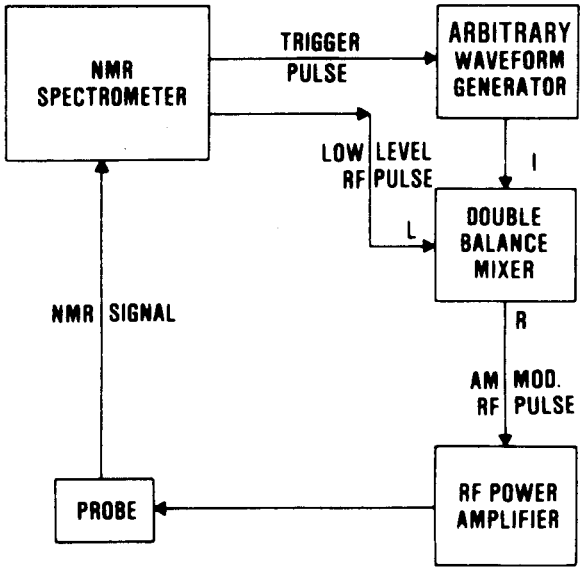

Figure 3: Spectrometer modifications required to provide frequency selective or shaped RF pulse operation.

stronger gradients. Figure 2 illustrates this modification. In actual construction, the three gradient coil assemblies, shown separated in Figure 2 for clarity, are superimposed and centered around the sample in the probe (Hall et al., 1986a). The gradient control board uses gating signals from the pulse programmer to switch the respective gradients on and off in the appropriate sequence to generate images. The amplitude of the gradients is controlled by the spectrometer shim coil circuitry as well as the gain of the amplifiers (e.g., Techron Model 7520).

A second modification to permit more versatile imaging is a provision for "shaping" the RF pulses applied to the sample (Temps and Brewer, 1984). Normally these are simple rectangular RF pulses that contain a band of RF frequencies centered on the oscillator frequency whose bandwidth is inversely related to the pulse length and whose amplitudes are governed by the relationship

$$F(\upsilon) = AT(\sin \pi\upsilon T)/\pi\upsilon T,$$

where A is the amplitude, υ is the frequency, and T is the pulse length. By shaping the RF pulse, the distribution of frequencies and the bandwidth can be controlled. The components needed for this modification are given in Figure 3. The arbitrary waveform generator (e.g., Wavetek Model 75) generates a signal of variable shape and controlled length. By applying this signal to the mixer (e.g., Minicircuits Model ZAD-1SH) simultaneously with the RF pulse, the amplitude of the RF pulse follows the programmed shape. This shaped pulse is then amplified and applied to the sample in the probe. Two important pulse shapes are the Gaussian and the $(\sin x)/x$. The Gaussian pulse generates a band of frequencies whose amplitude distribution is Gaussian (Bauer et al., 1984). The $(\sin x)/x$ shape generates a rectangular band of frequencies (Temps and Brewer, 1984).

The third modification was the construction of an imaging probe that could accommodate samples up to 32 mm in diameter. The probe contains the coil that generates the RF field and detects the signal from the sample. This coil size is about the maximum that can be used in our spectrometer to obtain a tuned circuit at the 270 MHz proton frequency. The probe is essentially a hollow tube with provisions to raise and lower the sample to image-selected cross sections of the core. The probe body contains tuning and impedance matching capacitors for adjustments to match different samples. This probe contains no provision for varying the sample temperature.

In NMRI, the pulse sequence must include provisions for switching the gradient coil currents on and off. This provision is not a part of normal NMR spectrometer operation. The pulse sequence in primary use today for NMRI applications is the SPINWARP sequence illustrated in Figure 4 (Dumoulin, 1987). Shown are the timed sequences for irradiating the sample with the shaped RF pulse (a Gaussian pulse shape is shown) and the order in which the gradients are switched on and off together with their relative amplitudes. Finally, the signal is acquired when the A/D converter is gated on.

The shaped RF pulse together with the Z-axis gradient, G_Z, defines a thin cross-sectional "slice" through the sample in which the spins are flipped and generate a signal. A stronger G_Z or a narrower bandwidth for the RF pulse will produce a thinner slice. The negative G_Z gradient after the RF pulse refocuses the spins following the dephasing caused by the positive G_Z gradient. A matrix containing information about the location of spins in the

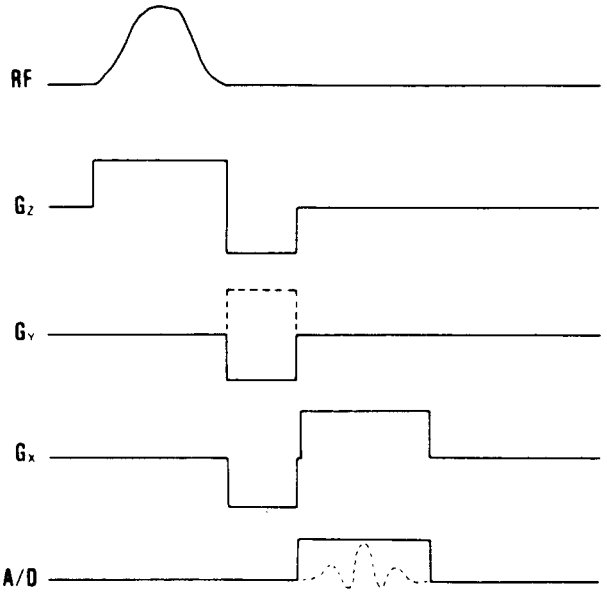

Figure 4: SPINWARP pulse sequence used for NMRI. (The horizontal dimension is time, increasing from left to right.)

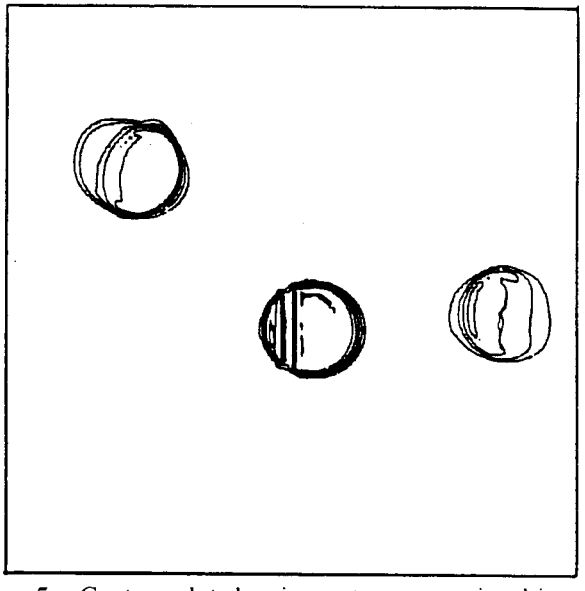

Figure 5: Contour plot showing water proton signal intensity as a function of X–Y position for a phantom consisting of three 4.3 mm i.d. water-filled NMR tubes.

Y-direction is acquired in successive steps by varying the amplitude of the G_Y gradient in fixed increments from the minimum to the maximum value in the imaging process. Finally, the signal is acquired while the G_X gradient is on, so that each signal contains information about the location of spins in the X-direction. By performing a two-dimensional Fourier transformation of this data matrix in both X and Y directions, a two-dimensional matrix of spin density as a function of frequency in both X and Y is obtained. Because the frequency is related to position by the presence of the linear gradients, the result is an image of the sample in terms of spin or proton density as a function of X–Y position across the sample.

APPLICATIONS

A cross-sectional contour plot of the NMR image of a phantom consisting of three water-filled NMR tubes (5 mm o.d., 4.3 mm i.d.) is shown in Figure 5. A phantom in NMRI is a simple arrangement of fluid-filled tubes used to check the performance of the system. The contours are at constant water proton signal intensity as a function of X–Y position. The glass in the tube walls produces no proton signal. A stack plot of the same phantom image is shown in Figure 6. In the stack plot each separate X-axis profile for the different G_Y values is plotted in successive order. The unequal amplitude of the signal as a function of X–Y position is partly caused by poor homogeneity of the RF coil magnetic field across the sample. In a true image of the sample, the signal intensity would be converted to a gray scale or false color scale and the separate pixels with their apparent color or gray level would be plotted as a function of position. This capability will be incorporated later in our system. In these images, 128 separate G_Y values were used with 128 points digitized in the G_X direction resulting in a resolution of 128 × 128 pixels.

The contour plot image obtained for a sandpack consisting of 25–30 mesh sand in a 16.5 mm i.d. test tube is shown in Figure 7. The sandpack was saturated with 1% NaCl brine. The slice imaged was approximately 3 mm thick as determined by the RF pulse bandwidth and the value of G_Z. The X–Y resolution was 128 × 128 pixels

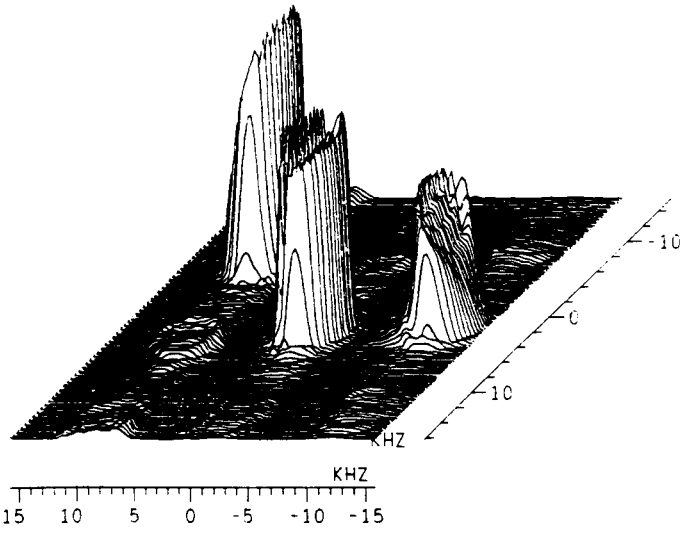

Figure 6: Stack plot of the data set shown in Figure 5. The vertical axis represents signal intensity.

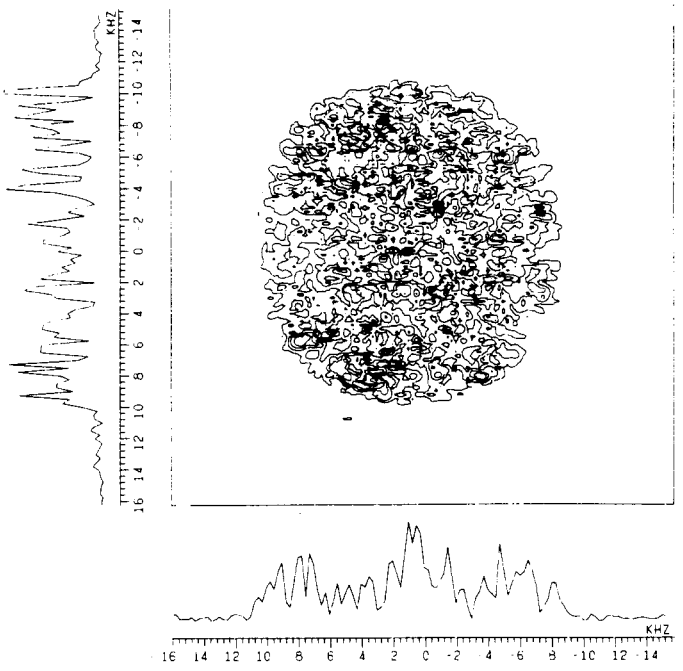

Figure 7: Contour plot of water signal intensity for a sandpack containing 1% NaCl brine. Also shown are intensity profiles through the center of the sandpack.

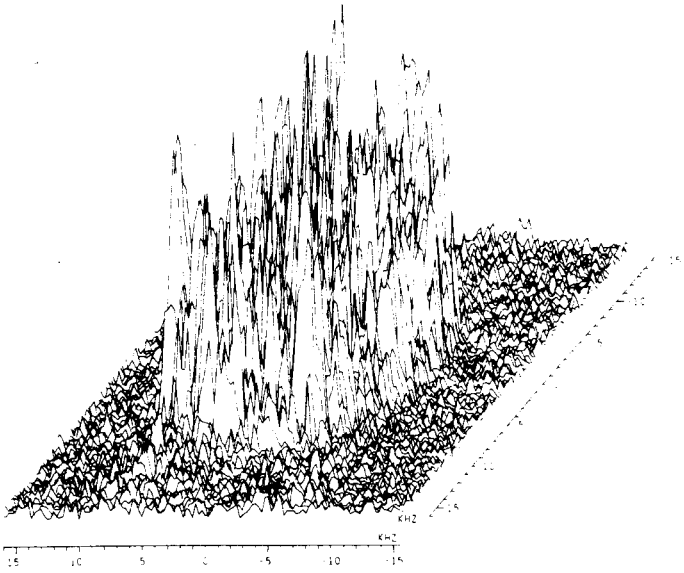

Figure 8: Stack plot of the data set shown in Figure 7.

as above. A stackplot of the same data is shown in Figure 8.

Berea and Cottage Grove sandstone plug samples (4 inches long by 1 inch diameter) were fitted with Lucite end caps and wrapped with epoxy-impregnated gauze. The end caps contain nylon tubing fittings for saturating the core samples. One of the end caps has a locator hole that fits on a pin in the sample support to precisely reposition the sample for repeated measurements.

Attempts to obtain images of the plug samples of Berea and Cottage Grove sandstone saturated with 1% NaCl brine were unsuccessful. No detectable signal was observed following the SPINWARP pulse sequence. The observed water signal using a simple 90° RF pulse without gradient switching had a very broad peak width of approximately 5,000 Hz for both samples. Preliminary tests on a smaller plug (¾ inch diameter) of Cleveland sandstone saturated in 1% NaCl brine showed a narrower water peak, and imaging experiments revealed some water signal around the outer region of the core. The T_1 and T_2 values for the Cottage Grove plug were measured using an inversion recovery sequence for T_1 and the Carr-Purcell-Meiboom-Gill spin echo sequence for T_2 (Harris, 1983). The measured value of T_1 was 287 milliseconds, and the value of T_2 was 0.794 milliseconds.

DISCUSSION OF THE RESULTS AND SIGNIFICANT OBSERVATIONS

Our preliminary results with the water phantoms and sandpack show that the basic modifications to the spectrometer to achieve NMRI capability work, but need some improvements. An unequal signal amplitude response with fall-off in the outer regions of the sample volume are revealed in Figures 5 and 6. Because of difficulty in obtaining a resonant circuit at 270 MHz over this large sample volume, the RF coil inductance was reduced by reducing the vertical dimensions of the RF coil from its ideal height-to-diameter ratio. This probably accounts for much of the poor RF field homogeneity and amplitude response. This problem could be alleviated either by reducing the spectrometer frequency (also requiring a reduction in magnetic field strength) or by going to smaller core sizes with a smaller RF coil diameter, which is not desirable for fluid flow studies.

The inability to image the plug samples can be explained by the broad proton signal and the extremely short T_2 value, which are inversely related. In a time interval of five T_2 periods, which would be 4 milliseconds for the Cottage Grove plug sample, the remaining signal would be negligible. The gradient coils have an apparent gradient rise and fall time of several milliseconds. Also, to obtain thin image slices in NMRI, an RF pulse with a narrow bandwidth is required, which means a pulse length of several milliseconds. Thus, the signal decays to zero before the required shaped RF pulse and field gradient switching have been completed. The width of signals from core fluids and their inversely related T_2 values tend to increase with spectrometer frequency because of the local magnetic field inhomogeneities that are caused by magnetic susceptibility differences between the fluid and rock particles (Glasel and Lee, 1974). The T_2 signal could be increased by reducing the magnetic field and operating at a lower frequency. Also, gradient coil designs having much shorter rise and fall times are available

(Mansfield and Chapman, 1986). However, these gradient systems tend to require more space within the magnet bore. All of the petrographic imaging studies published to date have been performed at frequencies much lower than 270 MHz.

Our plans involve obtaining a superconducting magnet power supply to enable us to reduce our magnetic field to operate at a lower frequency. We have constructed a new RF coil for the imaging probe that is more nearly ideal in its shape. This new coil and the tuning and matching circuitry operate at 60 MHz for protons. At this frequency, the new T_2 values should be more than 4 times longer, allowing ample time for gradient switching to image our plug samples. We are also adding multislice capability to our NMRI by building circuitry to shift the spectrometer frequency during the interval between the RF pulse and the detection period. Under current operation the frequency remains constant, and only a slice at the center of the RF coil is imaged. We are also considering obtaining a new gradient coil system having rise and fall times of 0.3 milliseconds, an order of magnitude better response than our current coil assembly.

SUMMARY

NMRI has shown potential in the past 2 years for investigating rock–fluid interactions, and newly reported developments suggest that more valuable applications are to come. By modifying an existing high-resolution NMR spectrometer for NMRI, imaging capability has been achieved at much lower cost than is possible with commercial instruments. Preliminary results on sandpacks and sandstone plug samples showed several areas where instrument operation must be modified to improve imaging performance for typical rock samples.

ACKNOWLEDGEMENTS

This work was supported in part by the Department of Energy under cooperative agreement DE-FC22-83FE60149. We particularly acknowledge the invaluable help of Dr. Tom Mareci of the University of Florida at Gainesville for providing the pulse gradient control board circuitry and NMRI references.

REFERENCES

Baldwin, B. A. and Yamanashi, W. X. (1986), "Detecting Fluid Movement and Isolation in Reservoir Cores Using Medical NMR Imaging Techniques," Presented at the Fifth SPE/DOE Symposium on Enhanced Oil Recovery, Tulsa, Oklahoma, 20–23 April 1986, SPE/DOE Paper 14884.

Bauer, C., Freeman, R., Frenkiel, T., Keeler, J., and Shaka, A. J. (1984), "Gaussian Pulses," *J. Magn. Reson.*, v. 58, p. 442.

Blackband, S. P., Mansfield, P., Barnes, J. R., Claque, A. D. H., and Rice, S. A. (1986), "Discrimination of Crude Oil and Water in Sand and Berea Cores with NMR Imaging," *SPE Formation Evaluation*, pp. 31–34, February 1986.

Dumoulin, C. L. (1987), "Nuclear Magnetic Resonance Imaging," *Spectroscopy*, v. 2, no. 1, p. 32.

Glasel, J. A. and Lee, K. H. (1974), "On the Interpretation of Water Nuclear Magnetic Resonance Relaxation Times in Heterogeneous Systems," *J. Amer. Chem. Soc.*, v. 96, p. 970.

Hall, L. D., Luck, S., and Rajanayagam, V. (1986a), "Construction of a High-Resolution NMR Probe for Imaging with Submillimeter Spatial Resolution," *J. Magn. Reson.*, v. 66, p. 349.

——— and Rajanayagam, V. (1987), "Thin-Slice, Chemical-Shift Imaging of Oil and Water in Sandstone Rock at 80 MHz," *J. Magn. Reson.*, v. 74, p. 139.

———, ———, and Hall, C. (1986b), "Chemical-Shift Imaging of Water and N-Dodecane in Sedimentary Rocks," *J. Magn. Reson.*, v. 68, p. 185.

Harris, R. K. (1983), *Nuclear Magnetic Resonance Spectroscopy*, London: Pitman Books Limited.

Lauterbur, P. C. (1973), "Image Formation by Induced Local Interactions: Examples Employing Nuclear Magnetic Resonance," *Nature*, v. 242, p. 190.

——— (1974), "Magnetic Resonance *Zeugmatography*," *Pure Appl. Chem.*, v. 40, p. 149.

Mansfield, P. and Chapman, B. (1986), "Active Magnetic Screening of Gradient Coils in NMR Imaging," *J. Magn. Reson.*, v. 66, p. 573.

Rothwell, W. P. and Vinegar, H. J. (1985), "Petrophysical Applications of NMR Imaging," *Applied Optics*, v. 24, p. 3969.

Saraf, D. N. and Fatt, I. (1965), "Three-Phase Relative Permeability Measurement Using a Nuclear Magnetic Resonance Technique for Estimating Fluid Saturation," *Soc. Pet. Eng. J.*, September, pp. 235–242.

Schmidt, E. J., Velasco, K. K., and Nur, A. M. (1986), "Quantifying Solid-Fluid Interfacial Phenomena in Porous Rocks with Proton Nuclear Magnetic Resonance," *J. Appl. Phys.*, v. 59, p. 2788.

Temps, A. J., Jr. and Brewer, C. F. (1984), "Synthesis of Arbitrary Frequency Domain Transmitting Pulses Applicable to Pulsed NMR Instruments," *J. Magn. Reson.*, v. 56, p. 355.

Volk, A., Tiffon, B., Mispelter, J., and Lhoste, J. M. (1987), "Chemical Shift-Specific Slice Selection. A New Method for Chemical Shift Imaging at High Magnetic Field," *J. Magn. Reson.*, v. 71, p. 168.